IFS #627

July 11, 1994

Toroidal plasma beta-finite Larmor radius limit in a toroidally linked mirror system

H. Vernon Wong, H.L. Berk, V.I. Ilgisonis[a]
and V.P. Pastukhov[a]
Institute for Fusion Studies, The University of Texas at Austin
Austin, Texas 78712

The ballooning stability limit in one toroidal section of the recently proposed toroidally linked neutron source is investigated within the framework of the Wentzel-Kramers-Brillouin (WKB) approximation. Rotational effects induced by radial electric fields present in the equilibrium are neglected. The equilibrium pressure and density profiles are taken to be linear in the flux variable. For a reasonable set of design parameters, ideal ballooning instability limits the toroidal plasma beta to less than 1%. However the inclusion of stabilizing kinetic effects due to finite ion Larmor radius approximately doubles the predicted critical beta limit, and makes possible a choice of design parameters compatible with ballooning stability.

PACS Nos.: 52.35.Py, 52.35.-g

I. INTRODUCTION

It has been suggested by Pastukhov and Berk[1] that a toroidally linked mirror system is advantageous as a basis of a neutron source for testing materials for a fusion reactor. Steady-state high-beta plasmas with energetic ions can be produced from beam-target plasmas in quadrupole mirror machines. Having a high-beta plasma is very important for achieving an intense source. However, in open mirrors, the electron temperature T_e may be low due to electron thermal losses along the field line. By linking the mirrors with toroidal sections to recirculate the plasma escaping the mirrors, higher electron temperatures can be achieved resulting in longer ion energy lifetimes and improvement in source power efficiency.

The flux surfaces at the ends of quadrupole mirrors are highly elliptical and can be matched smoothly to elliptical flux surfaces in the toroidal sections. It is envisaged that the vacuum toroidal magnetic fields have zero rotational transform. However, the particle orbits, despite the toroidal drifts, remain close to the flux surfaces due to the rotational flow induced by radial electric fields present in the equilibrium.

The pressure weighting of the hot ions in the good curvature regions of the quadrupole mirrors more than compensates the warm plasma pressure in the bad curvature regions of the toroidal sections to give a favorable sta-

[a]Permanent address: Institute of Nuclear Fusion, Russian Research Center "Kurchatov Institute," 123182 Moscow, Russia.

bility criterium to flute modes. However, the equilibrium can be unstable to ballooning modes in which the perturbations are finite in the toroidal sections where the field line curvature is unfavorable but decay to zero at the center of the mirror cells. In this paper, we investigate the limits on toroidal plasma beta due to short wavelength ballooning instabilities.[2] We include in our analysis the stabilizing effects of finite ion Larmor radius (FLR), and we evaluate the "finite-m" modifications of the conventional "infinite-m" ideal ballooning theory. We find appreciable improvement in the predicted stability due to FLR effects compared to ideal MHD theory.[3,4]

In Sec. II, we first consider the simplest case in which the perturbations are restricted to the toroidal connections and do not extend into the mirror cells. We derive the local dispersion relation for ballooning modes and the ray equations for the trajectories of energy propagation of these modes using a technique developed by Nevins and Pearlstein.[4] The ray orbits move in a four-dimensional phase space and satisfy Hamiltonian equations. For flux surfaces with large ellipticity, the orbits are separable into a fast motion nearly perpendicular to the flux surfaces and a slow azimuthal drift. We introduce a canonical transformation which effectively separates the fast and slow motion, and after evaluating the corresponding adiabatic invariants, we obtain a global dispersion relation by quantizing the adiabatic invariants. In Sec. III, we calculate and plot the critical plasma beta limits as a function of the ion Larmor radius.

The restriction of the perturbations to the toroidal connections assumes that it is energetically much less expensive to "bend" the field lines in the toroidal connections and requires for its validity $\log(E) \gg 1$, where E is the ellipticity of the elliptical flux surfaces. For realistic configurations, the ellipticity is $E \sim 12$ and $\log(E)$ is not particularly large compared to unity. In Sec. IV, we discuss the modifications introduced when perturbations extend into the mirror cells, and the most unstable perturbations now involve field-line bending in the mirror cells. The critical beta limits are reduced but finite FLR stabilizing effects can still be significant, and lead to stable predictions for appropriate design parameters.

In Sec. V, we compare the toroidal plasma beta of the proposed design parameters of Pastukhov and Berk[1] with the predicted values of critical beta for ballooning mode stability.

II. DISPERSION RELATION

Figure 1 is a schematic representation of the toroidally linked mirror configuration proposed by Pastukhov and Berk.[1] In the limit of zero beta, the flux surfaces are circular at the center of each quadrupole mirror but transform into highly elliptical shapes at the ends. The flux surfaces in the toroidal sections are therefore highly elliptical so that they can be matched smoothly to the elliptical surfaces at the mirror ends, and the ellipse is oriented with minor axis parallel to the toroidal radius of curvature.[1,5]

We may describe the plasma toroidal equilibrium in terms of coordinates (x, y, ζ) where x and y are Cartesian coordinates perpendicular to the toroidal axis and ζ is the toroidal angle (see Fig. 2).

The magnetic field B_0 in the toroidal section is taken to be

$$\mathbf{B}_0 = \frac{\hat{\zeta} B_t}{(1 + x/R_0)}$$

independent of the toroidal angle ζ. B_0 is the magnitude of the toroidal magnetic field and R_0 the field line radius of curvature on the magnetic axis. $\hat{\zeta}$ is the unit vector in the direction of increasing ζ.

In the limit of zero plasma beta, the toroidal flux surfaces are ellipses. We introduce the flux variable ψ given by

$$\psi = \psi_b \left(\frac{x^2}{\sigma^2} + \frac{y^2}{\tau^2} \right)$$

where $\psi =$ constant defines the elliptical flux surfaces σ and τ are the minor and major radius of the elliptical plasma surface $x^2/\sigma^2 + y^2/\tau^2 = 1$ located at $\psi = \psi_b \equiv B_t \sigma \tau / 2$. The ellipticity parameter $E \equiv \tau/\sigma \gg 1$ is very much greater than unity, with minor axis parallel to the radius of curvature. We neglect finite beta corrections to the equilibrium.

The x, y coordinates of the flux surfaces are:

$$\frac{x}{\sigma} = \left(\frac{\psi}{\psi_b} \right)^{1/2} \cos \theta_0$$

$$\frac{y}{\tau} = \left(\frac{\psi}{\psi_b} \right)^{1/2} \sin \theta_0$$

where θ_0 is the usual azimuthal angle coordinate in cylindrical geometry. The magnetic field B_0 can be represented in terms of field line flux variables ψ and $\theta(\psi, \theta_0)$

$$\mathbf{B}_0 = \nabla\psi \times \nabla\theta(\psi, \theta_0) = \hat{\zeta}\, B_t \frac{\partial\theta}{\partial\theta_0}$$

where

$$\nabla\psi = 2\psi_b \left(\frac{x}{\sigma^2}\,\hat{x} + \frac{y}{\tau^2}\,\hat{y}\right)$$

$$\nabla\theta_0 = \frac{\psi_b}{\sigma\tau\psi}\,(x\hat{y} - y\hat{x})$$

and the angular coordinate θ is determined by

$$\frac{\partial\theta}{\partial\theta_0} = \frac{1}{(1 + (\sigma/R_0)(\psi/\psi_b)^{1/2}\cos\theta_0)}$$

$\hat{x}$ and $\hat{y}$ are unit vectors in the direction of increasing x and y respectively, and

$$\hat{\zeta} = \hat{x} \times \hat{y}\,.$$

We assume $\sigma/R_0 \ll 1$, and we approximate B_0 and θ by:

$$\mathbf{B}_0 = \hat{\zeta}B_t \left(1 - \left(\frac{\sigma}{R_0}\right)\left(\frac{\psi}{\psi_b}\right)^{1/2} \cos\theta_+ \cdots\right)$$

$$\theta = \theta_0 + \cdots$$

We introduce the coordinate $\ell = (R_0 + x)\zeta \approx R_0\zeta + \cdots$, which measures distance along a field line, to complete the set of field line coordinates (ψ, θ, ℓ).

The stability analysis is most conveniently discussed in terms of these field line coordinates.

These flux variables are also appropriate for describing the low beta plasma equilibrium in the mirror cells. Inside the mirror cells the unit vector $\hat{\zeta}$ is constant, $\hat{\zeta} = \hat{z}$, and the flux surfaces are elliptical with ellipticity $E(z)$ varying with the z-coordinate. Finite beta effects which not only distort the elliptical flux surfaces but also shifts the magnetic axis are ignored. The field line coordinate ℓ now coincides with the z-coordinate to lowest order, $\ell = z$. The ellipticity is $E(\ell) = E \gg 1$ at $\ell = \pm\pi R_0/2$, where the mirror cells join with the toroidal connections, and decreases smoothly to $E(\ell) = 1$ at the center of the mirrors $\ell = \pm(\pi R_0/2 + L_m/2) \equiv \pm L_0$, where the flux surfaces become circular. L_m is the length of a mirror cell.

The ballooning mode equation may be obtained from the following variational quadratic form:

$$\int d^3r \left[\frac{(\mathbf{b}\cdot\nabla\phi)^2}{8\pi} |\mathbf{k}_\perp|^2 - \phi^2 \frac{\mathbf{b}\times\mathbf{k}_\perp\cdot\boldsymbol{\kappa}}{B_0} \frac{\mathbf{b}\times\mathbf{k}_\perp\cdot\nabla p_0}{B_0} \right.$$
$$\left. - \tfrac{1}{2}\phi^2|\mathbf{k}_\perp|^2 \frac{m_i N_{0i}}{B_0^2}\left(\omega^2 - \frac{\omega\omega_i^* S_\theta}{E}\right)\right] = 0 \qquad (1)$$

where the field perturbation Φ is expressed in the eikonal form:

$$\Phi = \phi(\psi,\theta,\ell)\, e^{iS} \; .$$

$\phi(\psi,\theta,\ell)$ is slowly varying in ψ and θ, $|\mathbf{k}_\perp|\phi \gg \partial\phi/\partial\psi,\ \partial\phi/\partial\theta$. The phase function $S(\psi,\theta)$ is independent of ℓ, and the perpendicular wavenumber is

$$\mathbf{k}_\perp = \nabla S = S_\psi \nabla\psi + S_\theta \nabla\theta$$

$$S_\psi = \frac{\partial S}{\partial \psi}$$

$$S_\theta = \frac{\partial S}{\partial \theta} \ .$$

The field variable Φ is related to the perturbed vector potential $\mathbf{A} = \mathbf{A}_\perp$ and the MHD displacement vector $\boldsymbol{\xi}_\perp$ by $\mathbf{A}_\perp = \xi_\perp \times \mathbf{B}_0 = \Phi\nabla S$. Thus the perturbed perpendicular magnetic field is $\delta\mathbf{B}_\perp = \partial\phi/\partial\ell\, \mathbf{b} \times \mathbf{k}_\perp e^{iS}$. We neglect magenetic compressibility (low beta approximation). We also neglect perturbations of the parallel electric field not only inside the plasma (MHD approximation) but also in the vacuum region between the plasma boundary and a conducting wall assumed to be located on a flux surface.

The first two terms represent respectively the stabilizing effect of field-line bending and the destabilizing effect of unfavorable field-line curvature. The third term represents plasma inertia and includes the stabilizing effects of finite FLR. The ballooning mode equation with finite FLR has been derived for mirror geometries by Newcomb[6] and for more general equilibrium geometries in the eikonal approximation by many authors including Berk*et al.*[7]

$\mathbf{b} = \frac{\mathbf{B}_0}{B_0} = \hat{\zeta}$ is the unit vector in the direction of the magnetic field, $\boldsymbol{\kappa} = \mathbf{b}\cdot\nabla\mathbf{b} = -\frac{\hat{x}}{R_0} + \cdots$ is the field line curvature, p_0 the total plasma pressure, N_{0i} the ion density, and m_i the ion mass. The frequency of the perturbation is ω and the ion diamagnetic drift frequency is

$$\omega_i^* = -\frac{cE}{eN_{0i}}\frac{\partial p_{0i\perp}}{\partial\psi} \sim \frac{cE}{eN_{0i}}\frac{p_{0i\perp}}{\psi_b} \sim \frac{\rho_i^2}{\sigma^2}\Omega_i$$

where $\Omega_i = eB_0/m_i c$ is the ion cyclotron frequency and $\rho_i = (2p_{0i\perp}/m_i N_{0i}\,\Omega_i^2)^{1/2}$ is the ion Larmor radius. ω_i^* is taken to be of the order of MHD growth rates $\omega \sim (2\rho_i^2/\sigma R_0)^{1/2}\Omega_i$. We ignore the "azimuthal" rotation induced by equilibrium radial electric fields present in the equilibrium. However, it should be pointed out that any rotational shear which develops may be strongly destabilizing and deserves further investigation.

Substituting for $\nabla\psi$ and $\nabla\theta$, we have:

$$\mathbf{k}_\perp\cdot\mathbf{k}_\perp = \frac{B_t\,S_\theta^2}{2\psi E}\left[E^2\,g_1^2\,(S_\psi,\psi,S_\theta,\theta) + g_2^2\,(S_\psi,\psi,S_\theta,\theta)\right]$$

$$\frac{\mathbf{b}\times\mathbf{k}_\perp\cdot\nabla p_0(\psi)}{B_0}\,\frac{\mathbf{b}\times\mathbf{k}_\perp\cdot\boldsymbol{\kappa}}{B_0} = -\frac{S_\theta^2}{\sigma R_0\,B_t E}\left(\frac{\psi_b}{\psi}\right)^{1/2} g_2\,(S_\psi,\psi,S_\theta,\theta)\,\frac{\partial p_0}{\partial\psi}$$

where

$$g_1\,(S_\psi,\psi,S_\theta,\theta) = \frac{2\psi\,S_\psi}{S_\theta}\cos\theta - \sin\theta$$

$$g_2\,(S_\psi,\psi,S_\theta,\theta) = \frac{2\psi\,S_\psi}{S_\theta}\sin\theta + \cos\theta\ .$$

To lowest order in the eikonal approximation $(\mathbf{b}\cdot\nabla\phi \ll |\mathbf{k}_\perp|\phi)$, $\nabla\times\delta\mathbf{B}_\perp = i\partial\phi/\partial\ell\mathbf{k}_\perp\cdot\mathbf{k}_\perp\mathbf{b}e^{iS}+\cdots$, and in the vacuum region where there is no current, we require $\mathbf{k}_\perp\cdot\mathbf{k}_\perp = 0$.

At the plasma boundary, the tangential component $\mathbf{b}\times\nabla\psi\cdot\delta\mathbf{E}_\perp/|\nabla\psi|$ of $\delta\mathbf{E}_\perp = i\frac{\omega}{c}\mathbf{A}_\perp$ and the normal component $\nabla\psi\cdot\delta\mathbf{B}_\perp/|\nabla\psi|$ of $\delta\mathbf{B}_\perp$ are continuous, and hence $\partial\Phi/\partial\theta$ and $\partial/\partial\theta\, \mathbf{b}\cdot\nabla\Phi$ are continuous. The jump in $\partial\Phi/\partial\psi$ is obtained by integrating across the plasma boundary the more exact non-eikonal equation for Φ which we take to be:

$$\frac{1}{8\pi}\mathbf{B}_0\cdot\nabla\frac{1}{B_0}\nabla_\perp^2\mathbf{b}\cdot\nabla\Phi+\nabla_\perp\cdot\frac{N_{0i}\,m_i}{2B_0^2}\left(\omega^2-\frac{\omega\omega_i^*\,S_\theta}{E}\right)\nabla_\perp\Phi$$

$$+\nabla\cdot\frac{\mathbf{k}\times\boldsymbol{\kappa}}{B_0}\frac{\mathbf{b}\times\nabla p_0\cdot\nabla\Phi}{B_0}=0\,.$$

We then obtain

$$\lim_{\epsilon\to 0}\left[\frac{\partial}{\partial\ell}\left\{\frac{\nabla\psi\cdot\nabla\psi}{B_0}\frac{\partial}{\partial\psi}+\frac{\nabla\psi\cdot\nabla\theta}{B_0}\frac{\partial}{\partial\theta}\right\}\frac{\partial\Phi}{\partial\ell}\right.$$

$$+\left\{\frac{4\pi N_{0i}\,m_i}{B_0^2}\left(\omega^2-\frac{\omega\omega_i^*\,S_\theta}{E}\right)\right\}\left\{\frac{\nabla\psi\cdot\nabla\psi}{B_0}\frac{\partial}{\partial\psi}+\frac{\nabla\psi\cdot\nabla\theta}{B_0}\frac{\partial}{\partial\theta}\right\}\Phi$$

$$\left.+\frac{4\pi\mathbf{b}\wedge\boldsymbol{\kappa}\cdot\nabla\psi}{B_0^2}\frac{\partial p_0}{\partial\psi}\frac{\partial\Phi}{\partial\theta}\right]_{\psi_b-\epsilon}^{\psi_b+\epsilon}=0\,. \qquad (2)$$

For ballooning modes, the perturbations are negligible at the center of the mirror cells where the pressure weighting of the energetic particles in the region of favorable field line curvature is strongly stabilizing. Thus the proper boundary condition on the field line dependence of the perturbations is $\phi=0$ at the center of the mirror cells.

However, in the remainder of this section and in Sec. III, we simplify the analysis by considering perturbations which are restricted to the toroidal connections, and in Sec. IV, we discuss the modifications introduced when perturbations extend into the mirror cells.

A toroidal section of the linked mirror system extends from $\zeta = -\pi/2$ to $\zeta = \pi/2$ and is connected smoothly at $\zeta = -\pi/2$ and $\zeta = \pi/2$ to quadrupole mirrors.

We consider perturbations which are restricted to this toroidal section and which vary sinusoidally along the field line:

$$\phi(\ell) = \phi_0 \cos \frac{\ell}{R_0}$$

$$\mathbf{b} \cdot \nabla\phi = -\frac{\phi_0}{R_0} \sin \frac{\ell}{R_0} \ .$$

Thus the variational quadratic form can be rewritten as follows:

$$\int d\psi\, d\theta \, \frac{S_\theta^2\, \phi_0^2}{32\psi\, E R_0}\, D(S_\psi, \psi, S_\theta, \theta, \omega) = 0 \tag{3}$$

where

$$d^3r = \frac{d\psi\, d\theta\, d\ell}{B_0}$$

$$D(S_\psi, \psi, S_\theta, \theta, \omega) = \left[E^2\, g_1^2\,(S_\psi, \psi, S_\theta\ \theta) + g_2^2\,(S_\psi, \psi, S_\theta\ \theta)\right]$$
$$\left[1 - \frac{4\pi m_i\, N_{0i}\, R_0^2}{B_t^2}\left(\omega^2 - \frac{\omega\omega_i^*\, S_\theta}{E}\right)\right] + g_2\,(S_\psi\, \psi, S_\theta, \theta)\ \frac{16\pi\, R_0}{\sigma\, B_t^2}\,(\psi\psi_b)^{1/2}\,\frac{\partial p_0}{\partial\psi} \ . \tag{4}$$

The local dispersion relation for ballooning modes is

$$D(S_\psi, \psi, S_\theta, \theta, \omega) = 0 \ . \tag{5}$$

If we consider the case of $\omega_i^* \to 0$, D is a function of the ratio S_ψ/S_θ but not of S_ψ and S_θ separately. Since we assume $E^2 \gg 1$, we obtain an approximate solution of the local dispersion relation by choosing perturbations for which $\frac{2\psi S_\psi}{S_\theta} = \tan\theta$ in order to minimize the bending energy. We then obtain for ω^2:

$$\omega^2 = \frac{B_t^2}{4\pi m_i N_{0i} R_0^2}\left[1 + \frac{2R_0}{\sigma}\frac{8\pi}{B_t^2}\frac{\partial p_0}{\partial\psi}(\psi\psi_b)^{1/2}\cos\theta\right] .$$

Let p_0 vary linearly with respect to ψ for $\psi < \psi_b$:

$$p_0 = \widehat{p}_0\left(1 - \frac{\psi}{\psi_b}\right)\Theta(\psi_b - \psi)$$

where Θ is a step function of its argument.

The pressure gradient $\partial p_0/\partial\psi$ is negative for $\psi_b > \psi > 0$, and if the magnitude of the plasma beta $\beta \equiv 8\pi\,\widehat{p}_0/B_t^2$ is greater than $\sigma/2R_0$ ($\beta > \sigma/2R_0$), ω^2 is negative on certain field lines and there is then instability.

The most unstable field lines are in the neighborhood of $\psi \sim \psi_b$ and $\theta \sim 0$ where the perturbations are characterized by $S_\psi/S_\theta \sim 0$, that is, $S_\theta \gg S_\psi$.

However, when S_θ is large, stabilizing kinetic effects proportional to ω_i^* can become appreciable and the magnitude of β can be significantly increased above $\sigma/2R_0$, the critical beta limit predicted by ideal ballooning theory.

To obtain a more accurate estimate of the critical value of beta β_c, it is necessary to derive a global dispersion relation. We accomplish this within the framework of the eikonal approximation. We note that the ray equations which determine the trajectories of mode energy propagation are:

$$\begin{aligned}
\frac{d\psi}{d\tau} &= \frac{\partial D}{\partial S_\psi} \\
\frac{d\theta}{d\tau} &= \frac{\partial D}{\partial S_\theta} \\
\frac{dS_\psi}{d\tau} &= -\frac{\partial D}{\partial \psi} \\
\frac{dS_\theta}{d\tau} &= -\frac{\partial D}{\partial \theta}
\end{aligned} \tag{6}$$

where τ is a "time" variable which parameterizes "distance" along the trajectory.

The ray equations are Hamiltonian and it will be convenient to use the language of Hamiltonian dynamics to describe the trajectory as a "particle orbit" determined by the "Hamiltonian" $D(S_\psi, \psi, S_\theta, \theta, \omega)$. (S_ψ, ψ) and (S_θ, θ) are pairs of canonical variables. The Hamiltonian D is two-dimensional, time-independent, and non-separable. The particle moves in a four-dimensional phase space restricted to the energy shell $D = 0$.

We derive a global dispersion relation by establishing the existence of adiabatic invariants of the motion and by appropriate quantization of these invariants. Nevins and Pearlstein[4] investigated ballooning modes in mirror equilibria with highly elliptical flux surfaces and observed that there is a separation in the characteristic time scales of the particle orbit. There is rapid motion directed generally parallel to $\nabla\psi$ superimposed on a slow precession in θ.

We can separate this rapid motion from the slow precession by transforming to a new set of canonical variables $P_\psi, Q_\psi, P_\theta, Q_\theta$ using the mixed generating function $G(\psi, P_\psi, \theta, P_\theta)$:

$$G(\psi, P_\psi, \theta, P_\theta) = E\left(\frac{\psi}{\psi_b}\right)^{1/2} P_\theta \sin\theta + \frac{\psi}{\psi_b} P_\psi \,. \tag{7}$$

The transformation equations relating $S_\psi, \psi, S_\theta, \theta$ to $P_\psi, Q_\psi, P_\theta, Q_\theta$ are:

$$\begin{aligned} Q_\psi &= \frac{\partial G}{\partial P_\psi} = \frac{\psi}{\psi_b} \\ Q_\theta &= \frac{\partial G}{\partial P_\theta} = E\, Q_\psi^{1/2} \sin\theta \\ S_\theta &= \frac{\partial G}{\partial \theta} = E\, Q_\psi^{1/2} P_\theta \cos\theta \\ S_\psi &= \frac{\partial G}{\partial \psi} = \frac{1}{\psi_b}\left(P_\psi + \frac{Q_\theta P_\theta}{2Q_\psi}\right) . \end{aligned} \tag{8}$$

The new Hamiltonian is

$$\begin{aligned} \widehat{D}(P_\psi, Q_\psi, P_\theta, Q_\theta, \omega) = D(S_\psi, \psi, S_\theta, \theta, \omega) = \left\{\frac{4Q_\psi P_\psi^2}{P_\theta^2} + \frac{\left(1 + \frac{2Q_\theta P_\psi}{E^2 P_\theta}\right)^2}{\left(1 - \frac{Q_\theta^2}{E^2 Q_\psi}\right)}\right\} \\ \left\{1 - \frac{4\pi\, m_i\, N_{0i}\, R_0^2}{B_t^2}\left(\omega^2 - \omega\omega_i^* Q_\psi^{1/2} P_\theta \left(1 - \frac{Q_\theta^2}{E^2 Q_\psi}\right)^{1/2}\right)\right\} \\ + \frac{16\pi\, R_0}{B_t^2\, \sigma}\frac{\partial p_0}{\partial Q_\psi} Q_\psi^{1/2} \frac{\left(1 + \frac{2Q_\theta P_\psi}{E^2 P_\theta}\right)}{\left(1 - \frac{Q_\theta^2}{E^2 Q_\psi}\right)^{1/2}} \end{aligned} \tag{9}$$

where we consider $\cos\theta > 0$.

The perpendicular wavenumber $\mathbf{k}_\perp$ expressed in terms of the new variables is:

$$\mathbf{k}_\perp = \frac{2P_\psi Q_\psi^{1/2}}{\sigma}\left(1 - \frac{Q_\theta^2}{E^2 Q_\psi}\right)^{1/2} \widehat{x} + \frac{1}{\sigma}\left(P_\theta + \frac{2P_\psi Q_\theta}{E^2}\right)\widehat{y} \,.$$

In the limit of large ellipticity $E^2 \gg 1$, we can expand D as a power series in $1/E^2$ to obtain:

$$\widehat{D} = \widehat{D}_0 + \widehat{D}_1 + \cdots \tag{10}$$

where

$$\widehat{D}_0(P_\psi, Q_\psi, P_\theta, \omega) = \left(\frac{4Q_\psi\, P_\psi^2}{P_\theta^2} + 1\right)\left(1 - \frac{4\pi\, m_i\, N_{0i}\, R_0^2}{B_t^2}\,\left(\omega^2 - \omega\omega_i^*\, Q_\psi^{1/2}\, P_\theta\right)\right)$$
$$+\ \frac{16\pi\, R_0}{\sigma B_t^2}\,\frac{\partial p_0}{\partial Q_\psi}\, Q_\psi^{1/2} \tag{11}$$

$$\widehat{D}_1(P_\psi, Q_\psi, P_\theta, Q_\theta, \omega) = -\frac{1}{E^2}\left(\frac{4Q_\psi\, P_\psi^2}{P_\theta^2} + 1\right)\frac{\left(4\pi m_i\, N_{0i}\, R_0^2\, \omega\omega_i^*\, P_\theta\, Q_\theta^2\right)}{2B_t^2\, Q_\psi^{1/2}}$$
$$+\ \frac{1}{E^2}\left(\frac{4Q_\theta\, P_\psi}{P_\theta} + \frac{Q_\theta^2}{Q_\psi}\right)\left(1 - \frac{4\pi\, m_i\, N_{0i}\, R_0^2}{B_t^2}\,\left(\omega^2 - \omega\omega_i^*\, Q_\psi^{1/2}\, P_\theta\right)\right.$$
$$\left. +\ \frac{8\pi\, R_0}{\sigma\, B_t^2}\,\frac{\partial p_0}{\partial Q_\psi}\, Q_\psi^{1/2}\right)$$

$\widehat{D}_0(P_\psi, Q_\psi, P_\theta, \omega)$ is a one-dimensional Hamiltonian describing orbits in the (P_ψ, Q_ψ) phase plane. The orbits move along lines of constant $\widehat{D}_0$, parameterized by constant values of P_θ.

$\widehat{D}_1$ describes higher order corrections. In particular, the frequency of motion in the (P_θ, Q_θ) phase plane is smaller than that in the (P_ψ, Q_ψ) phase plane by a factor of $1/E$. Thus, fast motion in the (P_ψ, Q_ψ) phase plane has effectively been separated from slower motion in the (P_θ, Q_θ) phase plane.

For a pressure profile p_0 linear in Q_ψ and constant density N_0:

$$p_0 = \widehat{p}_0(1 - Q_\psi)\Theta(1 - Q_\psi)$$

$$N_0 = \widehat{N}_0\,\Theta(1 - Q_\psi)$$

we obtain for $\widehat{D}_0$:

$$\widehat{D}_0 = \left(\frac{4Q_\psi\,P_\psi^2}{P_\theta^2} + 1\right)\left\{1 - \left(\Omega^2 - \Omega\Omega_i^*\,P_\theta\,Q_\psi^{1/2}\right)\Theta(1 - Q_\psi)\right\} - \overline{\beta}\,Q_\psi^{1/2}\Theta(1-Q_\psi) \tag{12}$$

where

$$\Theta(1 - Q_\psi) = \begin{cases} 1 & Q_\psi < 1 \\ 0 & Q_\psi > 1 \end{cases}$$

$$\overline{\beta} = \frac{16\pi\,\widehat{p}_0\,R_0}{\sigma B_t^2} = \frac{2\beta\,R_0}{\sigma}$$

$$\Omega = \frac{\omega\,R_0}{v_A}$$

$$v_A^2 = \frac{B_t^2}{4\pi\,m_i\,\widehat{N}_0}$$

$$\Omega_i^* = \frac{R_0\,c\,\widehat{p}_{0i\perp}\,E}{v_A\,e\,\widehat{N}_{0i}\,\psi_b} = \frac{\rho_i}{\sigma}\left(\frac{R_0}{2\sigma}\right)^{1/2}\,\overline{\beta}_{i\perp}^{1/2}$$

$$\rho_i = \frac{1}{\Omega_i}\left(\frac{2\widehat{p}_{0i\perp}}{m_i\,\widehat{N}_{0i}}\right)^{1/2} .$$

$\overline{\beta}$ is the plasma beta normalized with respect to the critical beta predicted by ideal ballooning theory.

Solving for P_ψ,

$$P_\psi^2 = -\frac{P_\theta^2}{4Q_\psi}\left\{1 - \frac{\overline{\beta} Q_\psi^{1/2}\Theta(1-Q_\psi) + \widehat{D}_0}{1 - \left(\Omega^2 - \Omega\Omega_i^* P_\theta Q_\psi^{1/2}\right)\Theta(1-Q_\psi)}\right\}$$

$$\equiv -V\left(Q_\psi, P_\theta, \widehat{D}_0, \Omega, \Omega_i^*, \overline{\beta}\right) \qquad (13)$$

where V is the "potential well" for motion in the (P_ψ, Q_ψ) phase plane. The WKB wave function is determined by solutions of P_ψ with $\widehat{D}_0 = 0$.

V varies with Q_ψ as shown in Fig. 3. A turning point occurs at $Q_\psi = Q_a$. Outside the plasma boundary $Q_\psi = 1$, we have $\mathbf{k}_\perp \cdot \mathbf{k}_\perp = 0$. Hence $P_\psi^2 = -P_\theta^2/4Q_\psi$ to lowest order and Φ is proportional to $e^{\pm|P_\theta|Q_\psi^{1/2}}$. We have assumed that

$$\frac{\overline{\beta}}{1 - \Omega^2 + \Omega\Omega_i^* P_\theta} > 1 \ .$$

When these inequalities are satisfied, the orbit is closed and the adiabatic invariant of the motion is

$$I_\psi\left(P_\theta, \widehat{D}_0, \Omega, \Omega_i^*, \overline{\beta}\right) = \oint P_\psi \, dQ_\psi = \frac{2P_\theta}{c_0^{1/2}} \int_{a_0}^1 d\xi \, \frac{(\xi - a_0)^{1/2}}{(1 + b_0\,\xi)^{1/2}}$$

$$= \frac{2P_\theta}{b_0\, c_0^{1/2}}\left[(1+b_0)^{1/2}(1-a_0)^{1/2} + \frac{(1+a_0\,b_0)}{2b_0^{1/2}}\,\ell n\left\{\frac{1 - \frac{b_0^{1/2}(1-a_0)^{1/2}}{(1+b_0)^{1/2}}}{1 + \frac{b_0^{1/2}(1-a_0)^{1/2}}{(1+b_0)^{1/2}}}\right\}\right] \qquad (14)$$

where the integral $\oint P_\psi \, dQ_\psi$ is taken over a complete orbit and

$$a_0 = \frac{1 - \Omega^2 - \widehat{D}_0}{\overline{\beta} - \Omega\Omega_i^* P_\theta} \qquad (15)$$

$$c_0 = \frac{1 - \Omega^2}{\overline{\beta} - \Omega\Omega_i^* P_\theta} \qquad (16)$$

$$b_0 = \frac{\Omega\Omega_i^* P_\theta}{(1-\Omega^2)} \tag{17}$$

The eikonal "wave function" is of the form $\Phi = \phi\, e^{iS(\psi,\theta)}$ where the phase factor S can be evaluated by integrating $\mathbf{k}_\perp = \nabla S$ along a ray trajectory and to lowest order is determined by motion in the (P_ψ, Q_ψ) plane:

$$S = \int_{\text{ray}} \nabla S \cdot d\mathbf{r} = \int P_\psi\, dQ_\psi + \int P_\theta\, dQ_\theta \approx \int P_\psi\, dQ_\psi + P_0\, Q_\theta$$

where $P_\theta = P_0$ a constant to lowest order and we neglect the higher order variations of P_θ which occur on a slower time scale than the fast motion in the (P_ψ, Q_ψ) phase plane.

The eikonal "wave function" Φ decays exponentially to the left of the turning point $Q_\psi = Q_a$ where $P_\psi = 0$:

$$\Phi \sim \phi e^{-\int_{Q_\psi}^{Q_a} |P_\psi| dQ_\psi}, Q_a > Q_\psi > 0\ .$$

The continuity of $\nabla\psi \cdot \delta\mathbf{B}_\perp$ and Φ across the plasma boundary imply that P_θ is continuous. We have and will hereafter omit the phase factor $e^{iP_0 Q_\theta}$ from the wavefunction Φ for convenience in notation, since it is a common factor present in Φ inside and outside the plasma boundary.

To the right of $Q_\psi = Q_a$, Φ has the form[8]

$$\Phi \sim \phi \sin\left(\int_{Q_a}^{Q_\psi} P_\psi\, d\psi + \frac{\pi}{4}\right)\ , \quad 1 > Q_\psi > Q_a\ .$$

In the neighborhood of the plasma boundary $Q_\psi = 1$, Φ has the form:

$$\Phi \sim \pm\, \phi \sin\left(\int_{Q_\psi}^{1} P_\psi dQ_\psi + \alpha_0\right)\ , \quad 1 > Q_\psi > Q_a\ .$$

If a conducting wall is placed at the plasma boundary, $\Phi = 0$ at $Q_\psi = 1$ and the phase $\alpha_0 = 0$.

If a conducting wall is located far away from the plasma boundary,

$$\Phi \sim \pm\, d_0 \phi e^{-|P_\theta|(Q_\psi^{1/2}-1)}\ , \qquad Q_\psi > 1\ .$$

Since $|P_\theta| > 1$ (except when the WKB approximation breaks down), Φ exponentially decays rapidly to zero outside the plasma boundary.

Φ is continuous at $Q_\psi = 1$, and the "jump" in $\partial\Phi/\partial Q_\psi$ is obtained from Eq. (2). Since $2\psi\, \partial\Phi/\partial\psi - \tan\theta\, \partial\Phi/\partial\theta = 2Q_\psi\, \partial\Phi/\partial Q_\psi$, we obtain to lowest order in $1/E^2$,

$$\lim_{\epsilon \to 0} \left[\frac{\partial}{\partial \ell} E \frac{\partial}{\partial \ell} \frac{\partial \Phi}{\partial Q_\psi} + \frac{4\pi N_{0i}\, m_i}{B_0^2} \left(\omega^2 - \omega\omega_i^*\, P_\theta\right) E\, \frac{\partial \Phi}{\partial Q_\psi} \right]_{Q_\psi = 1-\epsilon}^{Q_\psi = 1+\epsilon} .$$

With these boundary conditions, the phase α_0 and amplitude d_0 (with $\widehat{D}_0 = 0$) are determined by

$$\tan\alpha_0 = \frac{\left[2P_\psi(1 - \Omega^2 + \Omega\Omega_i^* P_\theta)\right]_{Q_\psi = 1-\epsilon}}{|P_\theta|} \tag{18}$$

$$d_0 = \sin\alpha_0$$

For compatibility of the eikonal "wave function" in the range $1 > Q_\psi > Q_a$, we require

$$\sin\left(\int_{Q_a}^{Q_\psi} P_\psi\, dQ_\psi + \frac{\pi}{4}\right) = \pm \sin\left(\int_{Q_\psi}^{1} P_\psi\, dQ_\psi + \alpha_0\right)\ ,$$

$$= \pm \sin\left[\left(\int_{Q_a}^{1} P_\psi\, dQ_\psi + \alpha_0 + \frac{\pi}{4}\right) - \left(\int_{Q_a}^{Q_\psi} P_\psi\, dQ_\psi + \frac{\pi}{4}\right)\right]$$

or

$$\int_{Q_a}^{1} P_\psi \, dQ_\psi + \frac{\pi}{4} + \alpha_0 = (n_1 + 1)\pi \ , \quad n_1 = 0, 1, 2, \ldots \ .$$

Thus the quantization condition to be imposed on I_ψ is

$$I_\psi = \oint P_\psi \, dQ_\psi = 2(n_1 + 1)\pi - \frac{\pi}{2} - 2\alpha_0 \ , \quad n_1 = 0, 1, 2, \ldots \ . \tag{19}$$

The most stable configuration would be to place the conducting wall at the plasma boundary so that $Q_w = 1$ and $\alpha_0 = 0$.

Equation (19) implicitly defines $\widehat{D}_0 = \widehat{D}_0(P_\theta, \Omega, \Omega_i^*, \overline{\beta})$ as a function of $P_\theta, \Omega, \Omega_i^*, \overline{\beta}$. The global dispersion relation for Ω, to lowest order in $1/E \ll 1$, is therefore given by

$$\widehat{D}_0(P_\theta, \Omega, \Omega_i^*, \overline{\beta}) = 0 \tag{20}$$

where P_θ is a parameter which we may conveniently choose to have the value $P_\theta = P_0$ such that the following subsidiary condition is satisfied:

$$\left. \frac{\partial \widehat{D}_0(P_\theta, \Omega, \Omega_i^*, \overline{\beta})}{\partial P_\theta} \right|_{P_\theta = P_0} = 0 \ . \tag{21}$$

Equations (20) and (21) are real functions of Ω. If Ω is a solution, so also is the complex conjugate Ω^*. Thus at marginal stability where $\Omega = \Omega_0$, Ω_0 is pure real ($\Omega_0 = \Omega_0^*$) and Ω_0 is a double root:

$$\left. \frac{\partial \widehat{D}_0(P_\theta, \Omega, \Omega_i^*, \overline{\beta})}{\partial \Omega} \right|_{\Omega = \Omega_0} = 0 \ . \tag{22}$$

Equations (20), (21), and (22) together determine the critical plasma beta $\overline{\beta}_c$ at marginal stability as a function of Ω_i^*.

The eikonal approximation is accurate if the magnitude of the decay exponent in the eikonal wave function

$$\Phi \sim \phi \exp\left(-\int_{Q_\psi}^{Q_a} |P_\psi| dQ\psi\right)$$

can be large in the region $Q_a > Q_\psi > 0$. Let us then define δ_x as

$$\delta_x \equiv \int_0^{Q_a} \left|P_\psi\left(Q_\psi, P_\theta, \widehat{D}_0 = 0, \Omega, \Omega_i^*, \overline{\beta}\right)\right| dQ_\psi = \frac{P_\theta}{c_0^{1/2}} \int_0^{c_0} d\xi \frac{(c_0 - \xi)^{1/2}}{(1 + b_0\,\xi)^{1/2}}$$

$$= P_\theta \left[-\frac{1}{b_0} + \frac{(1 + b_0\,c_0)}{2b_0^{3/2}\,c_0^{1/2}} \left(\frac{\pi}{2} - \sin^{-1}\frac{1 - b_0\,c_0}{1 + b_0\,c_0}\right)\right]. \tag{23}$$

We therefore require $\delta_x > 1$ to justify the validity of the WKB analysis.

To next order in $1/E^2$, we expand $\widehat{D}_0$ in a Taylor series about $P_\theta = P_0$ and $\Omega = \Omega_0$, and we obtain for $\widehat{D}$:

$$\widehat{D} = \frac{(\delta\Omega)^2}{2}\frac{\partial^2 \widehat{D}_0}{\partial \Omega_0^2} + \frac{(P_\theta - P_0)^2}{2}\frac{\partial^2 \widehat{D}_0}{\partial P_0^2} + \widehat{D}_1 + \cdots = 0 \tag{24}$$

where $\delta\Omega = \Omega - \Omega_0$.

The adiabatic invariant I_θ in the (P_θ, Q_θ) phase plane may be evaluated by approximating $\widehat{D}_1$ by its average over the fast motion in (P_ψ, Q_ψ) phase plane:

$$\widehat{D}_1 = \frac{\oint d\tau\, \widehat{D}_1(P_\psi, Q_\psi, P_0, Q_\theta, \Omega_0, \Omega_i^*, \overline{\beta})}{\oint d\tau} + \cdots = \frac{Q_\theta^2}{E^2}\overline{\widehat{D}_1} + \cdots \tag{25}$$

where

$$\overline{\widehat{D}_1} = \frac{\oint \frac{d\tau}{Q_\psi}\left\{\frac{\overline{\beta}\, Q_\psi^{1/2}(1 - \Omega_0^2)}{2(1 - \Omega_0^2 + \Omega_0\,\Omega_i^*\, P_0\, Q_\psi^{1/2})} + \left(1 - \Omega_0^2 + \Omega_0\,\Omega_i^*\, P_0\, Q_\psi^{1/2} - \overline{\beta}\, Q_\psi^{1/2}\right)\right\}}{\oint d\tau}$$

$$= \frac{1}{\oint d\tau}\left[\frac{P_0}{2}\left(\frac{\overline{\beta}}{(1-\Omega_0^2)} - \frac{(1+b_0\,c_0)}{c_0}\right)\left(\frac{\pi}{2} - \sin^{-1}\left(\frac{2c_0 + b_0\,c_0 - 1}{1+b_0\,c_0}\right)\right)\right.$$

$$\left. - \frac{P_0\,\overline{\beta}\,b_0(1-c_0)^{1/2}}{(1-\Omega_0^2)(1+b_0\,c_0)(1+b_0)^{1/2}} + \frac{P_0(1-c_0)^{1/2}(1+b_0)^{1/2}}{c_0^{1/2}}\right] \tag{26}$$

$$\oint d\tau = \frac{P_0}{2}\int_{Q_a}^{1}\frac{dQ_\psi}{Q_\psi^{1/2}}\,\frac{1}{\left(1-\Omega_0^2+\Omega_0\,\Omega_i^*\,P_0\,Q_\psi^{1/2}\right)^{1/2}\left(\overline{\beta}\,Q_\psi^{1/2} - \Omega_0\,\Omega_i^*\,P_0\,Q_\psi^{1/2} - 1 + \Omega_0^2\right)^{1/2}}$$

$$= \frac{P_0\,c_0^{1/2}}{(1-\Omega^2)b_0^{1/2}}\,\ell n\left\{\frac{1+b_0^{1/2}(1-c_0)^{1/2}/(1+b_0)^{1/2}}{1-b_0^{1/2}(1-c_0)^{1/2}/(1+b_0)^{1/2}}\right\}$$

Thus for Eq.(23), we have:

$$\frac{(\delta\Omega)^2}{2}\,\frac{\partial^2\widehat{D}_0}{\partial\Omega_0^2} + \frac{(P_\theta - P_0)^2}{2}\,\frac{\partial^2\widehat{D}_0}{\partial P_0^2} + \frac{Q_\theta^2}{E^2}\,\overline{\widehat{D}_1} + \cdots = 0 \tag{27}$$

The orbit in the (P_θ, Q_θ) phase plane is closed if

$$\overline{\widehat{D}_1}\,\frac{\partial^2\widehat{D}_0}{\partial P_0^2} > 0$$

in which case the adiabatic invariant I_θ is

$$I_\theta = \oint P_\theta\,dQ_\theta = \oint(P_\theta - P_0)dQ_\theta = \frac{-2\pi E\,\frac{(\delta\Omega)^2}{2}\,\frac{\partial^2\widehat{D}_0}{\partial\Omega_0^2}}{\left(2\overline{\widehat{D}_1}\,\frac{\partial^2\widehat{D}_0}{\partial P_0^2}\right)^{1/2}}\;. \tag{28}$$

The turning points in the (P_θ, Q_θ) phase plane occur at values of Q_θ where $(P_\theta - P_0) = 0$ and the appropriate quantization of I_θ is

$$I_\theta = 2(n_2+1)\pi - \pi = 2\left(n_2 + \tfrac{1}{2}\right)\pi\;, \quad n_2 = 0, 1, 2, \ldots\;. \tag{29}$$

Thus the frequency correction $\delta\Omega$ for $n_2 = 0$ is

$$(\delta\Omega)^2 = -\frac{1}{E}\frac{\left(2\overline{\widehat{D}_1}\,\frac{\partial^2 \widehat{D}_0}{\partial P_0^2}\right)^{1/2}}{\left(\frac{\partial^2 \widehat{D}_0}{\partial \Omega_0^2}\right)} . \tag{30}$$

III. MARGINAL STABILITY

A set of equations equivalent to Eqs. (20), (21), and (22), which may more conveniently be used to determine the critical plasma beta $\overline{\beta}_c$ at marginal stability, is the following:

$$I_\psi\left(P_0, \widehat{D}_0 = 0, \Omega_0, \Omega_i^*, \overline{\beta}_c\right) = \frac{3\pi}{2} - 2\alpha_0\left(P_0, \widehat{D}_0 = 0, \Omega_0, \Omega_i^*, \overline{\beta}_c\right) \tag{31}$$

$$\frac{\partial I_\psi}{\partial P_0} + 2\frac{\partial \alpha_0}{\partial P_0} = 0 \tag{32}$$

$$\frac{\partial I_\psi}{\partial \Omega_0} + 2\frac{\partial \alpha_0}{\partial \Omega_0} = 0 \tag{33}$$

where we consider the case of $n_1 = 0$ in the quantization condition for I_ψ.

A. Let us first assume the conducting wall to be at the plasma boundary so that $\psi_w = \psi_b$ and $\alpha_0 = 0$.

a. In the limit of $\Omega_i^* \ll \frac{16}{9(3)^{1/2}\pi}$, we may verify a posteriori that $9\pi/8P_0 \ll 1$ and $b_0 = \frac{\Omega\Omega_i^* P_0}{1-\Omega^2} \ll 1$. We can then approximate Eq. (14) for I_ψ by:

$$I_\psi\left(P_0, \widehat{D}_0 = 0, \Omega_0, \Omega_i^*, \overline{\beta}_c\right) = \frac{4P_0}{3c_0^{1/2}}(1 - c_0)^{3/2} + \cdots \tag{34}$$

where for convenience we repeat Eq. (16) for c_0:

$$c_0 = \frac{1 - \Omega_0^2}{\overline{\beta}_c - \Omega_0\, \Omega_i^*\, P_0} \; .$$

From Eq. (31), we have

$$\frac{P_0 (1 - c_0)^{3/2}}{c_0^{1/2}} = \frac{9\pi}{8}$$

while from Eqs. (32) and (33)

$$\begin{aligned} (1 + 2c_0) c_0\, \Omega_0\, \Omega_i^*\, P_0 &= 2(1 - c_0)(1 - \Omega_0^2) \\ \Omega_0 &= \frac{c_0\, \Omega_i^*\, P_0}{2} \; . \end{aligned}$$

Thus

$$c_0 = 1 - \left(\frac{9\pi}{8P_0} \right)^{2/3} + \cdots \tag{35}$$

and we obtain for P_0 and Ω_0

$$P_0 = \left[\left(\frac{9\pi}{8} \right)^{2/3} \frac{4}{3\Omega_i^{*^2}} \left(1 - \Omega_i^{*^2} \frac{P_0^2}{4} \right) \right]^{3/8} = (3\pi^2)^{1/8} / \Omega_i^{*^{3}/4} + \cdots \tag{36}$$

$$\Omega_0 = \frac{\Omega_i^*\, P_0}{2} + \cdots = \tfrac{1}{2}\, (3\pi^2)^{1/8}\, \Omega_i^{*^{1}/4} \; . \tag{37}$$

Substituting for P_0 and Ω_0 in Eqs. (16) and (35), we have for $\overline{\beta}_c$:

$$\begin{aligned} \overline{\beta}_c &= \frac{(1 - \Omega_0^2)}{\left(1 - \left(\frac{9\pi}{8P_0} \right)^{2/3} \right)} + \Omega_0\, \Omega_i^*\, P_0 = 1 - \Omega_0^2 + \Omega_0\, \Omega_i^*\, P_0 + \left(\frac{9\pi}{8P_0} \right)^{2/3} + \cdots \\ &= 1 + (3\pi^2)^{1/4}\, \Omega_i^{*^{1}/2} \; . \end{aligned} \tag{38}$$

The magnitude of the decay exponent δ_x (Eq. (23)) is:

$$\delta_x = \frac{2P_0}{3} + \cdots = \frac{2}{3}\, (3\pi^2)^{1/8}\, \frac{1}{\Omega_i^{*^{3}/4}} \tag{39}$$

To obtain the frequency correction $\delta\Omega$, we calculate:

$$\frac{\partial^2 \widehat{D}_0}{\partial \Omega_0^2} = -\left[\frac{\partial^2 I_\psi}{\partial \Omega_0^2} \Big/ \frac{\partial I_\psi}{\partial \widehat{D}_0}\right]_{\widehat{D}_0=0} \approx -2$$

$$\frac{\partial^2 \widehat{D}_0}{\partial P_0^2} = -\left[\frac{\partial^2 I_\psi}{\partial P_0^2} \Big/ \frac{\partial I_\psi}{\partial \widehat{D}_0}\right]_{\widehat{D}_0=0}$$

$$\approx \frac{5\Omega_0\,\Omega_i^*}{3P_0} = \frac{5}{6}\Omega_i^{*2}$$

$$\overline{\widehat{D}_1} \approx \frac{\overline{\beta}}{2}\,.$$

Thus, for $n_2 = 0$, we obtain from Eq. (30) and Eq. (37)

$$\frac{(\delta\Omega)^2}{\Omega_0^2} = \left(\frac{100}{27\pi^2}\right)^{1/4} \frac{\overline{\beta}^{1/2}\,\Omega_i^{*1/2}}{E}\,. \tag{40}$$

b. Equations (31), (32), and (33) with $\alpha_0 = 0$, have been solved numerically to determine Ω_i^* for different values of $\overline{\beta}_c$. In Fig. 4, we plot $\overline{\beta}_c$ as a function of Ω_i^*. $\overline{\beta}_c = 1$ when $\Omega_i^* = 0$, and $\overline{\beta}_c$ increases with increasing Ω_i^*. Equation (38) for $\overline{\beta}_c$ is within 10% of the numerical result for $\Omega_i^* \lesssim 0.1$.

We also calculate numerically the decay exponent δ_x and the frequency correction

$E^{1/2}\,\delta\Omega/\Omega_0$, and these are plotted as a function of $\Omega_i^{*1/2}$ in Fig. 5. When $\Omega_i^* < .3155$, $\delta_x > 1$ and $\delta\Omega/\Omega_0 < 1$ (note that $E \gg 1$), and hence the eikonal approximation and the expansion of D in $1/E^2$ are justifiable. When $\Omega_i^* > .3155$, the orbit in the (P_θ, Q_θ) phase plane determined by Eq. (27)

is not closed ($\overline{D}_1\, \partial^2 \widehat{D}_0/\partial P_0^2$ is negative), and the expansion procedure is no longer valid.

Since $\Omega_i^* = (\rho_i/\sigma)(R_0/2\sigma)^{1/2}\overline{\beta}_{i\perp}^{1/2}$, if we assume the ion plasma beta is equal to the electron plasma beta $\left(\overline{\beta}_i = \overline{\beta}_e\right)$ and we take $\overline{\beta}_{i\perp} = \frac{1}{4}\overline{\beta}_c$, we can plot $\overline{\beta}_c$ as a function of $(\rho_i/\sigma)(R_0/2\sigma)^{1/2}$. We do this in Fig. 6. $\overline{\beta}_c = 2.4$ when $(\rho_i/\sigma)(R_0/2\sigma)^{1/2} = .25$.

B. If the conducting wall is far from the plasma boundary so that $\psi_w \to \infty$, we may approximate α_0 by Eq. (18). We solve numerically Eqs. (31), (32), and (33) for this case, and in Fig. 4, we also plot the variation of the critical beta $\overline{\beta}_c$ as a function of Ω_i^*. We plot the corresponding dependence of the decay exponent δ_x and the frequency correction $E^{1/2}\,\delta\Omega/\Omega_0$ on ${\Omega_i^*}^{1/2}$ in Fig. 5, and the dependence of $\overline{\beta}_c$ on the parameter $(\rho_i/\sigma)(R_0/2\sigma)^{1/2}$ (assuming $\overline{\beta}_i = \overline{\beta}_c$) in Fig. 6.

This configuration is less stable than that with the conducting wall at the plasma boundary. The magnitude of the critical beta $\overline{\beta}_c$ is smaller for a given value of $(\rho_i/\sigma)(R_0/2\sigma)^{1/2}$. For example, $\overline{\beta}_c$ is $\sim$ 15% smaller when $(\rho_i/\sigma)(R_0/2\sigma)^{1/2} \sim .25$.

IV. MODIFICATION DUE TO PERTURBATIONS EXTENDING INTO MIRROR CELLS

In this section, we discuss perturbations extending into the mirror cells. We impose the boundary condition that $\phi(\ell)$ is zero at the center of neighboring mirror cells, $\ell = \pm L_0 \equiv \pm(\pi R_0/2 + L_m/2)$, where the pressure weighting of the energetic particles in the region of favorable field-line curvature is strongly stabilizing.

We ignore field-line curvature in the mirror cells, and we model the variation of ellipticity $E(\ell)$ along the field line by an exponential function

$$E(\ell) = \begin{cases} \exp\left\{ \dfrac{(\ell + L_0)}{\ell_0} \right\} , & -\dfrac{\pi R_0}{2} > \ell > -L_0 \\[2ex] \exp\left\{ \dfrac{(L_0 - \ell)}{\ell_0} \right\} , & L_0 > \ell > \dfrac{\pi R_0}{2} \,. \end{cases}$$

Thus $E(\ell) = 1$ at the center of the mirror cells, $\ell = \pm L_0$ and $E(\ell) = E$ at the junction with the toroidal connection ($\ell = \pm \pi R_0/2$). The parameter ℓ_0 is related to E by $1/\ell_0 = (2/L_m) \log E$.

Let us consider the case of $\omega_i^* = 0$. As in Sec. II, we minimize the bending energy in the toroidal connection by choosing perturbations for which $2\psi S_\psi / S_\theta = \tan\theta$. At marginal stability where $\omega = 0$, we have for the quadratic form $L(\phi, \phi)$:

$$L(\phi,\phi) = \int d\psi d\theta \int_{-L_0}^{+L_0} d\ell \, \frac{S_\theta^2}{16\pi\psi E(\ell)\cos^2\theta} \left(\frac{\partial\phi}{\partial\ell}\right)^2$$

$$+ \int d\psi d\theta \int_{-\pi R_0/2}^{+\pi R_0/2} d\ell \, \frac{S_\theta^2 (\psi\psi_b)^{1/2}}{\sigma R_0 \, B_t^2 \psi E \cos\theta} \, \frac{\partial p_0}{\partial\psi} \, \phi^2 \,. \qquad (41)$$

Inside the toroidal connection where $E(\ell) = E$, the extremizing function $\phi(\ell)$ (the solution of the Euler-Lagrange equation obtained by taking the first variation of $L(\phi, \phi)$ with respect to ϕ) is:

$$\phi(\ell) = \frac{\cos \ell/R_1}{\cos \pi R_0/2R_1}\,, \qquad \frac{\pi R_0}{2} > \ell > -\frac{\pi R_0}{2} \tag{42}$$

where

$$\frac{1}{R_1^2} = -\frac{16\pi(\psi\psi_b)^{1/2}}{\sigma R_0\, B_t^2}\,\frac{\partial p_0}{\partial\psi}\,\cos\theta \tag{43}$$

Inside the mirror cells, the extremizing function is:

$$\phi(\ell) = \frac{2\log E}{L_m(E-1)}\int_{-L_0}^{\ell} d\ell E(\ell)\,, \qquad -\frac{\pi R_0}{2} > \ell > -L_0\,. \tag{44}$$

$\phi(\ell)$ is considered to be symmetric about the point $\ell = 0$, and it is sufficient to focus on ℓ in the range $0 > \ell > -L_0$. $\phi(\ell)$ is continuous and normalized to unity at $\ell = -\pi R_0/2$. For continuity of $\partial\phi/\partial\ell$ at $\ell = -\pi R_0/2$, we require:

$$\frac{1}{R_1}\tan\frac{\pi R_0}{2R_1} = \frac{2E\log E}{L_m(E-1)}\,. \tag{45}$$

This equation relates the value of R_1 to the equilibrium parameters and the criterion for marginal stability is then determined by Eq. (43). For p_0 varying linearly with ψ, the critical beta is

$$\beta_c = \frac{\sigma}{2R_0}\left(\frac{R_0}{R_1}\right)^2\,. \tag{46}$$

The critical beta is reduced by a factor of $(R_0/R_1)^2$ below that predicted by the ideal ballooning mode theory discussed in Sec. II for perturbations restricted to the toroidal connection. For large values of $(\pi R_0/L_m)\log E \gg R_1$, R is approximately given by

$$R_1 = R_0 + \delta R_1$$

$$\frac{\delta R_1}{R_0} = \frac{L_m(E-1)}{\pi R_0 E \log E} \ll 1 \; .$$

If $E = 12$ and $2R_0/L_m = 1$, the solution of Eq. (45) is $\pi R_0/2R_1 = 1.279$ and the critical beta is $2R_0/\sigma\beta_c = (R_0/R_1)^2 = .663$, a considerable reduction from previous estimates.

It is instructive to note that Eqs. (43) and (45) can also be obtained by substituting Eqs. (42) and (44) for $\phi(\ell)$ in the quadratic form [Eq. (41)]. If we then take R_1 to be a variational parameter, it may be verified that Eq. (45) for R_1 (that is, continuity of $\partial\phi/\partial\ell$ at $\ell = -\pi R_0/2$) extremizes the quadratic form, and we obtain:

$$L(\phi,\phi) = \int d\psi d\theta \frac{S_\theta^2(\pi R_0 + R_1 \sin \pi R_0/R_1)}{32\pi\psi E\cos^2 \pi R_0/2R_1 \cos^2\theta}\left[\frac{1}{R_1^2} + \frac{16\pi(\psi\psi_b)^{1/2}}{\sigma R_0 B_t^2}\frac{\partial p_0}{\partial\psi}\cos\theta\right] = 0.$$

Equating the expression inside the square brackets to zero yields Eq. (43).

Let us now consider the case of finite ω_i^*. Inside the mirror cells, the extremizing function is approximated by

$$\phi(\psi,\theta,\ell) = \int_{-L_0}^{\ell} d\ell \, \frac{B_0(\ell)}{|\mathbf{k}_\perp(\ell)|^2} \Big/ \int_{-L_0}^{-\pi R_0/2} d\ell \, \frac{B_0(\ell)}{|\mathbf{k}_\perp(\ell)|^2} \, , \quad -\frac{\pi R_0}{2} > \ell > -L_0 \; . \tag{47}$$

We ignore terms proportional to the equilibrium field-line curvature and we neglect the inertia terms. The ratio of the inertia term to the field-line bending term is

$$\frac{\text{inertia}}{\text{field} - \text{line bending}} \sim \left(\frac{\omega L_m}{2v_A \log E}\right)^2 .$$

We are interested in the parameter regime where $(1/\log E)^2 \ll 1$ and $\omega L_m/2v_A < 1$ at marginal stability.

In the toroidal connection

$$\phi = \frac{\cos \ell/R_1}{\cos \pi R_0/2R_1} , \qquad \frac{\pi R_0}{2} > \ell > -\frac{\pi R_0}{2} . \tag{48}$$

ϕ is continuous and equal to unity at $\ell = -\pi R_0/2$. For $\partial\phi/\partial\ell$ continuous at $\ell = -\pi R_0/2$, we require R_1 to be given by:

$$\begin{aligned}\frac{R_0}{R_1} \tan \frac{\pi R_0}{2R_1} &= \frac{R_0}{\left[\frac{|\mathbf{k}_\perp(\ell)|^2}{B_0(\ell)}\right]_{\ell=-\pi R_0/2}} \int_{-L_0}^{-\pi R_0/2} \frac{d\ell\, B_0(\ell)}{|\mathbf{k}_\perp(\ell)|^2} \\ &= \frac{L_m(1+\chi^2 E^2)}{2\chi E \log E} \left(\tan^{-1}\chi E - \tan^{-1}\chi\right)\end{aligned} \tag{49}$$

where

$$\chi \equiv \chi(P_\psi, \psi, p_\theta, \theta) = \frac{g_1(P_\psi, \psi, P_\theta, \theta)}{g_2(P_\psi, \psi, P_\theta, \theta)} .$$

If we substitute Eqs. (47) and (48) in Eq. (1) for the variational quadratic form $L(\phi, \phi)$, and we recognize that the value of R_1 (treated as a variational parameter) which extremizes $L(\phi,\phi)$ is given by Eq. (49), we obtain:

$$L(\phi,\phi) = \int d\psi d\theta\, \frac{S_\theta^2(1 + (R_1/\pi R_0) \sin \pi R_0/R_1)}{16\pi E R_0(1 + \cos \pi R_0/R_1)} D^+(S_\psi, \psi, S_\theta, \theta, \omega) = 0$$

where

$$D^+(S_\psi, \psi, S_\theta, \theta, \omega) = \left\{\frac{R_0^2}{R_1^2} - \frac{R_0^2}{v_A^2}\left(\omega^2 - \frac{\omega\omega_i^* S_\theta}{E}\right)\right\} g_1(S_\psi, \psi, S_\theta, \theta)$$

$$+\frac{16\pi R_0(\psi\psi_b)^{1/2}}{\sigma B_t^2}\, g_2(S_\psi,\psi,S_\theta,\theta)\,\frac{\partial p_0}{\partial\psi} \tag{50}$$

and D^+ differs from D defined by Eq. (4) through the presence of the ratio $(R_0/R_1)^2$ (instead of unity). The local dispersion relation is therefore:

$$D^+(S_\psi,\psi,S_\theta,\theta,\omega)=0$$

with R_0/R_1 determined by Eq. (49).

Transforming to new variables $P_\psi, Q_\psi, P_\theta, Q_\theta$ defined by Eq. (8), and expanding as a power series in $1/E^2$ as described in Sec. II, we obtain for D^+:

$$\begin{aligned} D^+(S_\psi,\psi,S_\theta,\theta,\omega) &= \widehat{D}^+(P_\psi,Q_\psi,P_\theta,Q_\theta,\Omega) \\ &= \widehat{D}_0^+(P_\psi,Q_\psi,P_\theta,\Omega)+\widehat{D}_1^+(P_\psi,Q_\psi,P_\theta,Q_\theta,\Omega)+\cdots \end{aligned}$$

where

$$\begin{aligned} \widehat{D}_0^+(P_\psi,Q_\psi,P_\theta,\Omega) &= \left(\frac{4Q_\psi P_\psi^2}{P_\theta^2}+1\right)\left\{\frac{R_0^2}{R_1^2}-\left(\Omega^2-\Omega\Omega_i^* P_\theta Q_\psi^{1/2}\right)\Theta(1-Q_\psi)\right\} \\ &\quad -\overline{\beta}Q_\psi^{1/2}\Theta(1-Q_\psi) \end{aligned} \tag{51}$$

while for Eq. (49) we have:

$$\frac{R_0}{R_0}\tan\frac{\pi R_0}{2R_1}=\frac{\frac{4R_0Q_\psi^{1/2}P_\psi}{L_m P_\theta}\log E}{\left(1+\frac{4Q_\psi P_\psi^2}{P_\theta^2}\right)\left(\tan^{-1}\frac{2Q_\psi^{1/2}P_\psi}{P_\theta}-\tan^{-1}\frac{2Q_\psi^{1/2}P_\psi}{P_\theta E}\right)}\,. \tag{52}$$

Equations (51) and (52) determine $P_\psi(Q_\psi,P_\theta,\widehat{D}_0^+,\Omega,\Omega_i^*,\overline{\beta})$. The phase factor which appears in the quantization condition (Eq. (18)) imposed on the adiabatic invariant $I_\psi = \oint P_\psi d\partial_\psi$ is given by (for a conducting wall far away):

$$\tan \alpha_0 = \left\{ \frac{\left[P_\psi \left(1 - \frac{R_1^2}{R_0^2}\left(\Omega^2 - \Omega\Omega_i^* P_\theta\right)\right)\right]}{|P_\theta|} Q_\psi = 1 - \epsilon \right\} . \tag{53}$$

We evaluate numerically the adiabatic invariant $I_\psi = \oint P_\psi dQ_\psi$ and we follow the procedure described in Sec. II to determine the critical beta $\overline{\beta}_c$ at marginal stability as a function of Ω_i^* and the FLR parameter $(\rho_i/\sigma)(R_0/2\sigma)^{1/2}$, using Eqs. (31), (32), and (33).

In Figs. 4 and 6 we plot the dependence of $\overline{\beta}_c$ on Ω_i^* and $(\rho_i/\sigma)(R_0/2\sigma)^{1/2}$ respectively for values of $E = 12$ and $2R_0/L_m = 1$. The lower values of $\overline{\beta}_c$ obtained (compared to Sec. III) reflect the fact that the most unstable perturbations involve some field-line bending in the mirrors. For the chosen values of E and $2R_0/L_m$, $\overline{\beta}_c$ is reduced by approximately 1/3. The fractional increase in $\overline{\beta}_c$ due to FLR effects, relative to the corresponding critical beta predicted in the ideal ballooning limit, are approximately the same for perturbations restricted to the toroidal connection and perturbations extending into the mirror cells.

The calculations discussed so far were based on an equilibrium profile in which the pressure varies linearly in ψ but the density is constant. They have been repeated for a somewhat more realistic equilibrium profile in which the pressure and density vary linearly in ψ (implying constant temperature):

$$p_0 = \widehat{p}_0(1 - Q_\psi)\Theta(1 - Q_\psi)$$

$$N_0 = \widehat{N}_0(1 - Q_\psi)\Theta(1 - Q_\psi) .$$

Equation (52) is then modified to be:

$$\widehat{D}(P_\psi, Q_\psi, P_\theta, Q_\theta, \omega) = \left(\frac{4Q_\psi P_\psi^2}{P_\theta^2} + 1\right)\left\{\frac{R_0^2}{R_1^2} - \left(\Omega^2(1-Q_\psi) - \Omega\Omega_i^* P_\theta Q_\psi^{1/2}\right)\Theta(1-Q_\psi)\right\}$$
$$- \overline{\beta} Q_\psi^{1/2} \Theta(1 - Q_\psi) \ . \qquad (54)$$

In Fig. 7 we plot the dependence of $\overline{\beta}_c$ on $(\rho_i/\sigma)(R_0/2\sigma)^{1/2}$ for values of $E = 12$ and $2R_0/L_m = 1$. The decay exponent $\delta_x < 1$ is less than unity for values of $(\rho_i/\sigma)(R_0/2\sigma)^{1/2} > .31$ and the eikonal approximation becomes inaccurate.

The stabilizing FLR effects are stronger for constant temperature profiles compared to constant density profiles, and the corresponding critical beta values are slightly larger.

V. DISCUSSION

We have investigated the ballooning stability limit in one toroidal section of a toroidally-linked mirror configuration taking into account finite Larmor radius effects. Equilibrium pressure and density profiles linear in the flux variable ψ were considered. Finite beta deformations of the equilibrium configuration and rotational effects induced by equilibrium "radial" electric fields were neglected. The most unstable ballooning mode perturbations are finite not only in the toroidal connection but extend into the mirror cells.

The critical beta predicted by ideal ballooning mode theory is given by Eq. (46):

$$\left(\frac{2R_0}{\sigma}\right)\beta_c = \left(\frac{R_0}{R_1}\right)^2$$

where R_0/R_1 is determined by Eq. (45):

$$\frac{R_0}{R_1}\tan\frac{\pi R_0}{2R_1} = \frac{2R_0 E\log E}{L_m(E-1)} .$$

The modification due to the stabilizing kinetic effects of finite FLR are determined by numerically evaluating the adiabatic invariant

$$I_\psi = \oint P_\psi(Q_\psi, P_\theta, \widehat{D}_0^+ = 0, \Omega_i, \Omega_i^*, \overline{\beta})dQ_\psi ,$$

where $P_\psi(Q_\psi, P_\theta, \widehat{D}_0^+ = 0, \Omega_i, \Omega_i^*, \overline{\beta})$ is obtained from Eq. (51) (or Eq. (54)), and then numerically solving Eqs. (31), (32), and (33). The results are presented in Figs. 6 and 7.

When stabilizing kinetic effects due to finite FLR are included, the magnitude of the critical beta relative to the ideal ballooning critical beta limit is approximately increased by a factor of ~ 2 for values of the FLR parameter $(\rho_i/\sigma)(R_0/2\sigma)^{1/2} \sim .02$. This enhancement allows one of the two specific designs discussed in Ref. 2 (and reproduced in Tables I and II) to achieve stability.

In the first set of design parameters presented in Table I, the mirror ratio is $R_m = 2$, and the toroidal elliptical flux surface has minor radius $\sigma = a/(R_m E)^{1/2} = 2.86\,\text{cm}$, major radius $\tau = a(E/R_m)^{1/2} = 34.3\,\text{cm}$. The ion Larmor radius in the toroidal section is $\rho_i = .14\,\text{cm}$.

The ellipticity is $E = 12$ and $2R_0/L_m = 1$. Ideal ballooning mode analysis predicts a critical beta limit of $\overline{\beta}_c = (R_0/R_1)^2 \approx .663$ or $\beta_c \approx .0047$ for the above design parameters. The magnitude of the parameter $(\rho_i/\sigma)(R_0/2\sigma)^{1/2}$ is 0.29. Assuming $\beta_i = \beta_e$, we note from Fig. 6 that stabilizing FLR effects increase the critical beta to $\overline{\beta}_c \sim 1.63$ (or $\beta_c \sim .012$) for conducting wall at the plasma boundary and $\overline{\beta}_c \sim 1.34$ (or $\beta_c \sim .01$) for a conducting wall at infinity. Thus we predict a critical beta limit which is lower than the design toroidal plasma beta of $\beta_t = .018$. We quote the results obtained with a constant density profile. Slightly larger values of β_c are predicted for a constant temperature profile.

In an alternative set of design parameters, the magnitude of the parameters a, B_t, and β_t, was changed to new values listed in Table II while all the others remained the same.

For these parameters the mirror ratio is $R_m = 2.25$, and the elliptical toroidal flux surface has minor radius $\sigma = 3.85$ cm, major radius $\tau = 46.2$ cm. The ion Larmor radius in the toroidal section is $\rho_i = .12$ cm.

The design toroidal plasma beta of $\beta_t = .01$ exceeds the critical beta limit of $\beta_c = .0064$ predicted by ideal ballooning for the second set of design parameters. The magnitude of $(\rho_i/\sigma)(2R_0/\sigma)^{1/2}$ is .16, and we note from Fig. 6 that the predicted critical beta ranges from $\overline{\beta}_c \sim 1.27$ (or $\beta_c \sim .012$) for a conducting wall at the plasma boundary to $\overline{\beta}_c \sim 1.13$ (or $\beta_c \sim .011$) for a conducting wall at infinity. Thus, when stabilizing FLR effects are included in the analysis, we predict a critical beta of $\sim .011$ which is slightly larger than the design toroidal plasma beta of $\beta_t = .01$.

ACKNOWLEDGMENTS

The authors would like to thank L.D. Pearlstein for emphasizing the importance of ballooning mode stability of the linked mirror concept, and also T.B. Kaiser and L.L. Lodestro for useful discussions during the course of this investigation.

References

[1]V.P. Pastukhov and H.L. Berk, Nucl. Fusion **10**, (1993).

[2]J.W. Conner, R.J. Hastie, and J.B. Taylor, Phys. Rev. Lett. **40**, 396 (1978); and Proc. R. Soc. London Ser. A **365** 1 (1970); A. Glasser, in *Proceedings of the Finite Beta Theory Workshop*, Varenna, Italy (U.S. Department of Energy, Washington, DC, 1979), p. 55; Y.C. Lee and J.W. Van Dam in *Proceedings of the Finite Beta Theory Workshop*, Varenna, Italy (U.S. Department of Energy, Washington, DC, 1979), p. 93.

[3]R.L. Dewar, J. Manickam, R.C. Grimm, and M.S. Chance, Nucl. Fusion **21**, 493 (1981).

[4]W.M. Nevins and L.D. Pearlstein, Phys. Fluids **31**, 1988 (1988).

[5]V.I. Ilgisonis, H.L. Berk, and V.P. Pastukhov, to be published in Phys. Fluids (1993).

[6]W.A. Newcomb, Phys. Fluids **28**, 505 (1985).

[7]H.L. Berk, M.N. Rosenbluth, H.V. Wong, T.M. Antonsen, and D.E. Baldwin, Sov. J. Plasma Phys. **9**, 108 (1983).

[8]L.D. Landau and E.M. Lifshitz, in *Quantum Mechanics* (Pergamon Press, London, 1959), p. 163.

Table I

Magnetic mirror		
	central magnetic field	$B_0 = 4\,\mathrm{T}$
	radius of central flux surface	$a = 15\,\mathrm{cm}$
	mirror cell length	$L_m = 400\,\mathrm{cm}$
Toroidal section		
	magnetic field	$B_t = 8\,\mathrm{T}$
	radius of curvature	$R_0 = 200\,\mathrm{cm}$
	electron temperature	$T_e = 2\,\mathrm{keV}$
	ion (tritium) temperature	$T_i = 2\,\mathrm{keV}$
	plasma beta	$\beta_t = .018$
	flux surface ellipticity	$E = 12$

Table II

radius of central flux surface	$a = 20\,\mathrm{cm}$
toroidal magnetic field	$B_t = 9\,\mathrm{T}$
toroidal plasma beta	$\beta_t = .01$

FIGURE CAPTIONS

Fig. 1. Schematic diagram of toroidally linked mirror configuration.

Fig. 2. x and y are Cartesian coordinates perpendicular to the toroidal axis and ζ is the toroidal angle.

Fig. 3. $V(Q_\psi)$ is the "potential well" for motion in (P_ψ, Q_ψ) phase plane.

Fig. 4. Variation of normalized critical beta $\overline{\beta}_c = 2\beta\, R_0/\sigma$ with $\Omega_i^* = (\rho_i/\sigma)(R_0/2\sigma)^{1/2}\overline{\beta}_{ic\perp}^{1/2}$ for constant density profile; (1) perturbation restricted to toroidal section, (2) perturbation extending from toroidal section into mirror cell.

Fig. 5. Variation of decay exponent δ_x and frequency correction $E^{1/2}\,\delta\Omega/\Omega_0$ with $\Omega_i^{*1/2}$ for constant density profile.

Fig. 6. Variation of normalized critical beta $\overline{\beta}_c = 2\beta\, R_0/\sigma$ with the Larmor radius parameter $(\rho_i/\sigma)(R_0/2\sigma)^{1/2}$ assuming $\overline{\beta}_{ic\perp} = \frac{1}{4}\,\beta_c$ for constant density profile; (1) perturbation restricted to toroidal section, (2) perturbation extending from toroidal section into mirror cell.

Fig. 7. Variation of normalized critical beta $\overline{\beta}_c = 2\beta\, R_0/\sigma$ with the Larmor radius parameter $(\rho_i/\sigma)(R_0/2\sigma)^{1/2}$ assuming $\overline{\beta}_{ic\perp} = \frac{1}{4}\,\beta_c$ for constant temperature profile; perturbation extending from toroidal section into mirror cell.

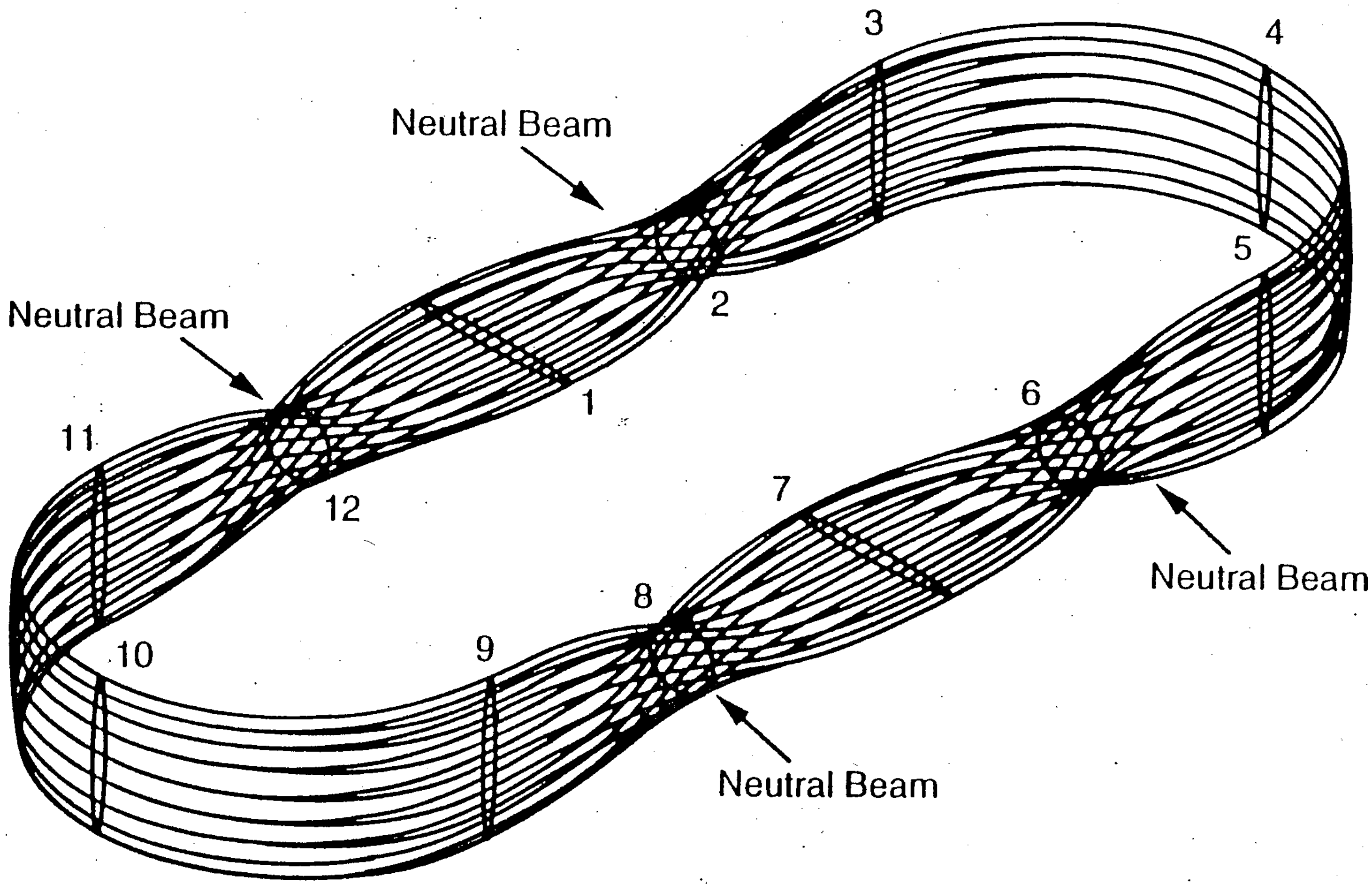

Neutral Beam
Neutral Beam
Neutral Beam
Neutral Beam
1
2
3
4
5
6
7
8
9
10
11
12

Figure 1

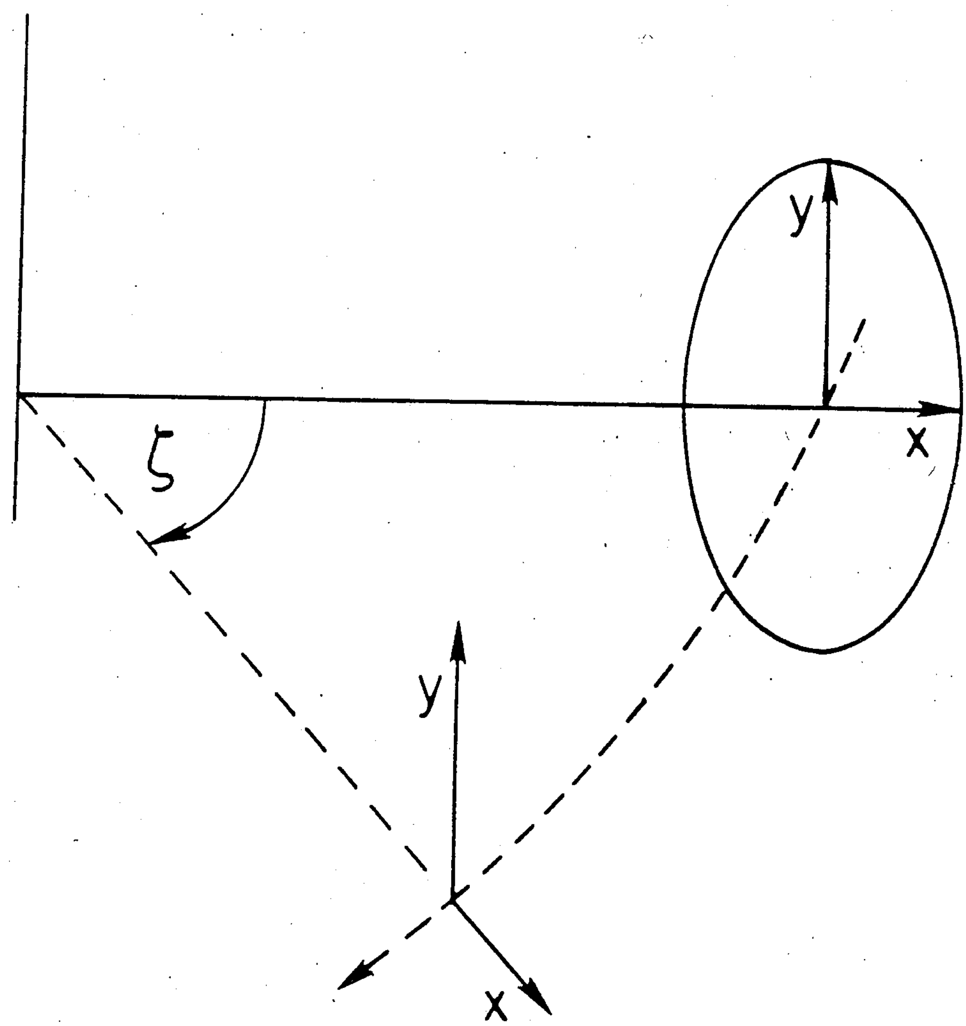

Fig. 2

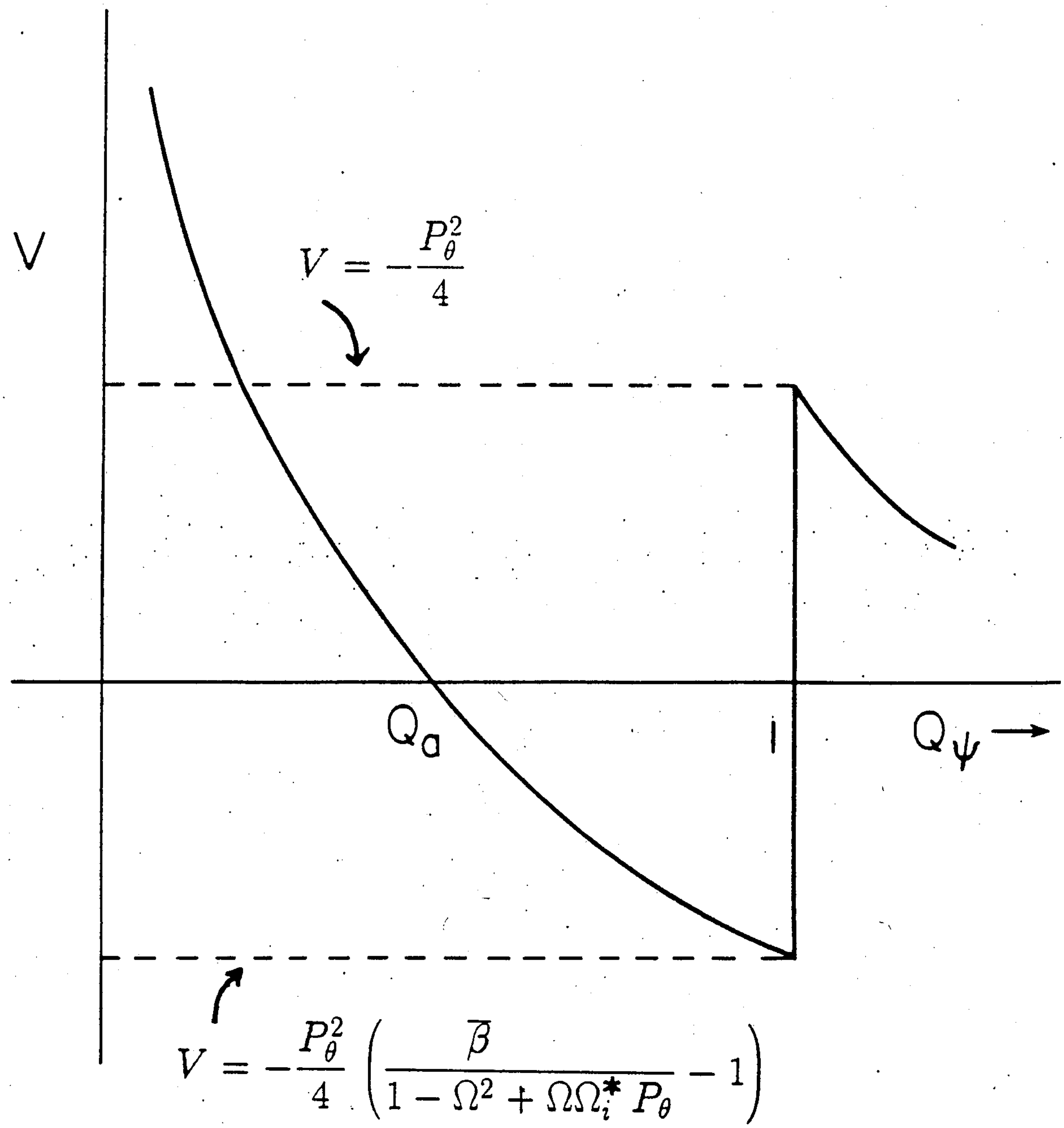
V
$V = -\frac{P_\theta^2}{4}$
Q_a
1
Q_ψ
$V = -\frac{P_\theta^2}{4}\left(\frac{\overline{\beta}}{1-\Omega^2+\Omega\Omega_i^* P_\theta}-1\right)$

Fig. 3

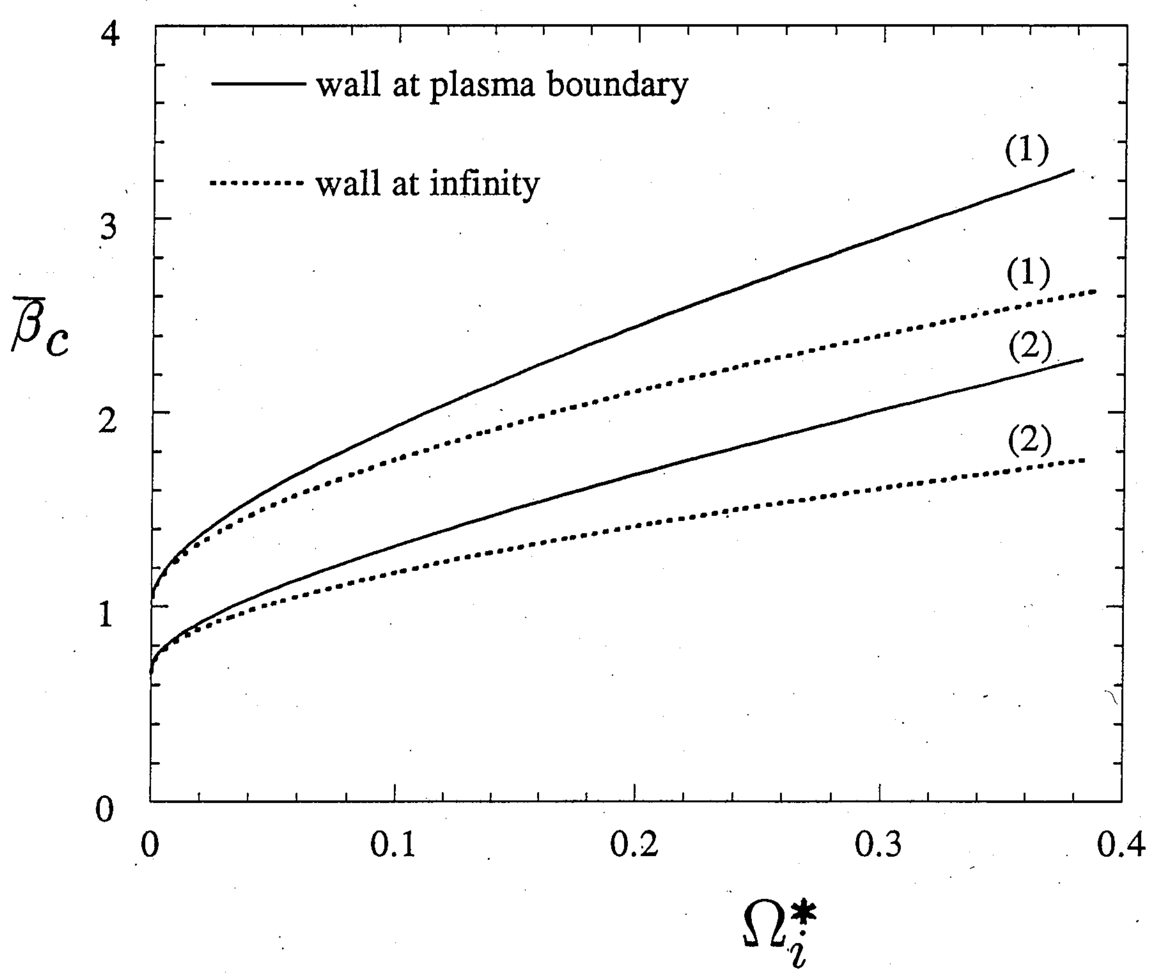
wall at plasma boundary
wall at infinity
(1)
(1)
(2)
(2)
$\overline{\beta}_c$
Ω_i^*
0
1
2
3
4
0
0.1
0.2
0.3
0.4

Fig. 4

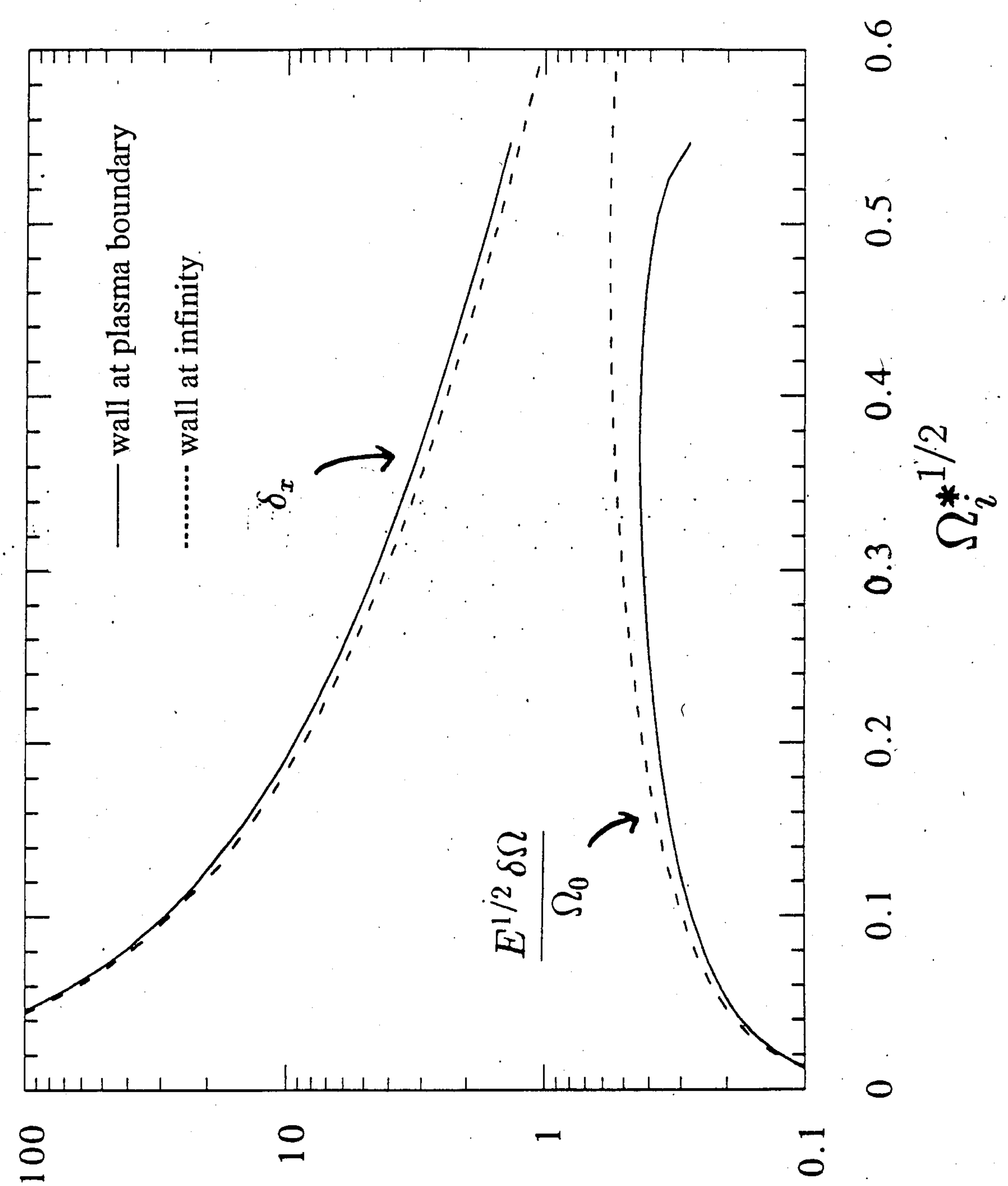

wall at plasma boundary
wall at infinity
δ_x
$\frac{E^{1/2}\delta\Omega}{\Omega_0}$
100
10
1
0.1
0
0.1
0.2
0.3
0.4
0.5
0.6
$\Omega_i^{*1/2}$

Fig. 5

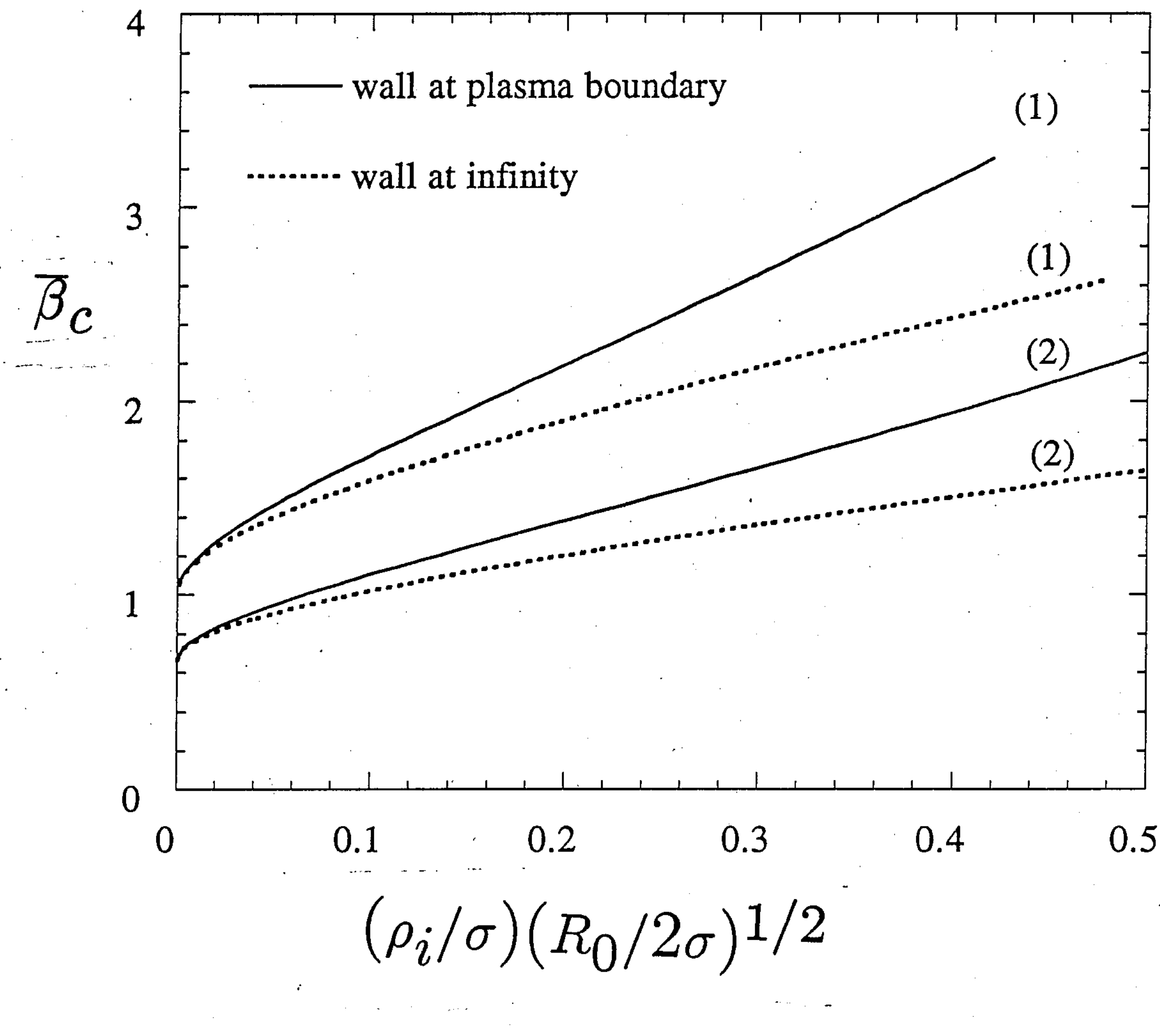

wall at plasma boundary
wall at infinity
(1)
(1)
(2)
(2)
4
3
2
1
0
$\overline{\beta}_c$
0
0.1
0.2
0.3
0.4
0.5
$(\rho_i/\sigma)(R_0/2\sigma)^{1/2}$

Fig. 6

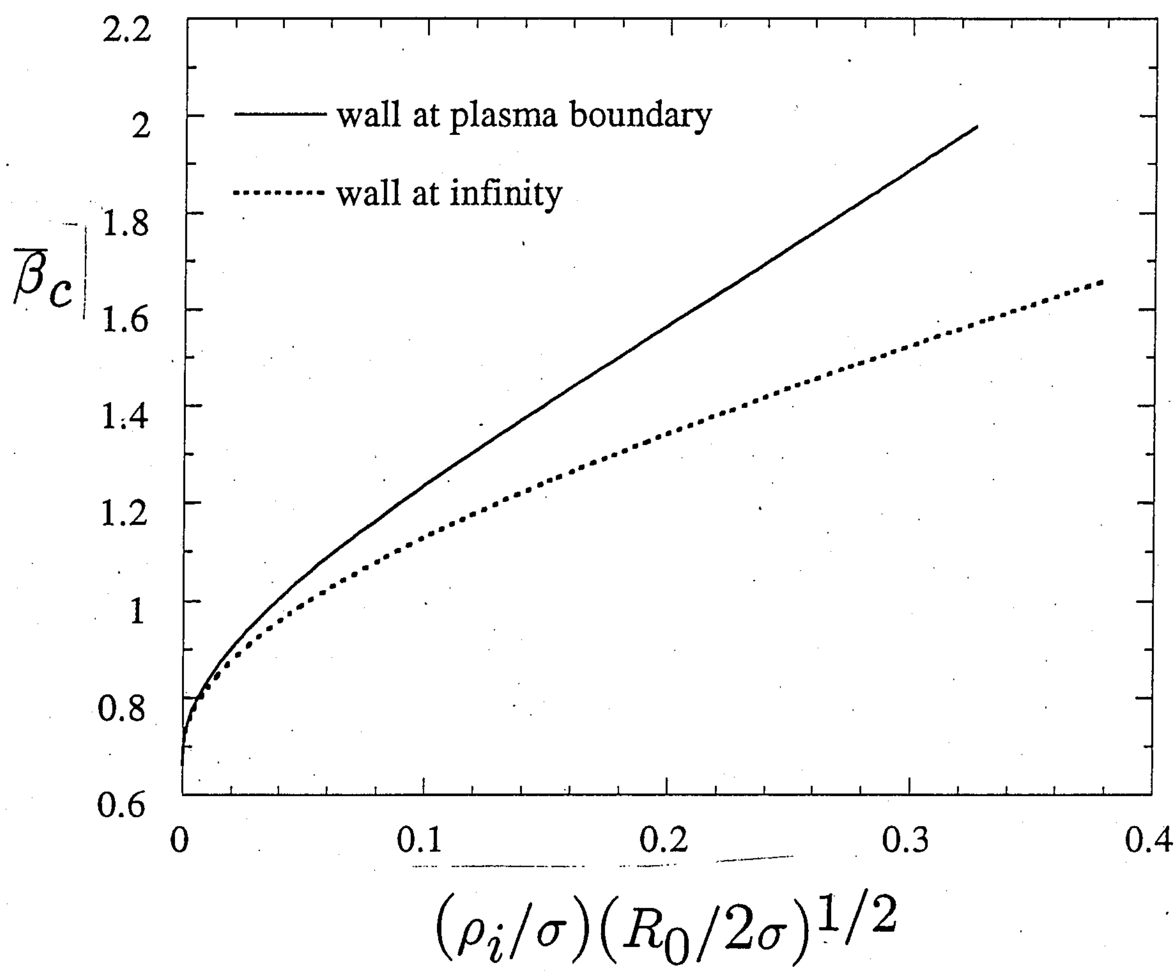

wall at plasma boundary
wall at infinity
$\overline{\beta}_c$
2.2
2
1.8
1.6
1.4
1.2
1
0.8
0.6
0
0.1
0.2
0.3
0.4
$(\rho_i/\sigma)(R_0/2\sigma)^{1/2}$

Fig. 7